New Journal of Physics
The open-access journal for physics

Aharonov–Bohm-like oscillations in Fabry–Perot interferometers

H Choi[1], P Jiang[1,2], M D Godfrey[1], W Kang[1,5], S H Simon[3], L N Pfeiffer[4], K W West[4] and K W Baldwin[4]

[1] James Franck Institute and Department of Physics, University of Chicago, Chicago, IL 60637, USA
[2] Department of Physics, National Taiwan Normal University, Taipei, Taiwan
[3] Rudolf Peierls Centre for Theoretical Physics, 1 Keble Road, Oxford University, OX1 3NP, UK
[4] Department of Electrical Engineering, Princeton University, Princeton, NJ 08544, USA
E-mail: wkang@uchicago.edu

New Journal of Physics **13** (2011) 055007 (9pp)
Received 26 January 2011
Published 24 May 2011
Online at http://www.njp.org/
doi:10.1088/1367-2630/13/5/055007

Abstract. An experimental study of a Fabry–Perot interferometer in the quantum Hall regime reveals Aharonov–Bohm-like (ABL) oscillations. Unlike the Aharonov–Bohm effect, which has a period of one flux quantum, Φ_0, ABL oscillations possess a flux period of Φ_0/f, where f is the integral value of fully filled Landau levels in the constrictions. The detection of ABL oscillations is limited to the low magnetic field side of the $\nu_c = 1, 2, 4, 6, \ldots$, integer quantum Hall plateaus. These oscillations can be understood within the Coulomb-dominated model of quantum Hall interferometers as forward tunneling and backscattering, respectively, through the center of the interferometer from the bulk and the edge states.

[5] Author to whom any correspondence should be addressed.

© IOP Publishing Ltd and Deutsche Physikalische Gesellschaft

Contents

1. Introduction

The possibility of realizing topologically protected qubit in the fractional quantum Hall (FQH) effect has kindled considerable interest in the study of interferometry in quantum Hall systems. The proposed topological quantum computation [1, 2] seeks to take advantage of the exotic quasiparticle statistics of the FQH states found at fillings $\nu = 5/2$ [3–5] and $12/5$ [5]. Theoretical studies have shown that the quasiparticles for these FQH states possess a non-locality, and the unitary representation of the exchange statistics is non-Abelian [6, 7]. The physical properties of a group of non-Abelian quasiparticles depend only on the topology of the braids, resulting in intrinsic fault tolerance.

Experimental confirmation of the non-Abelian statistics of the $\nu = 5/2$ FQH state can in principle be performed with Aharonov–Bohm interferometry of quasiparticles [2, 8, 9]. In the proposed experiments, adiabatic transport of a mobile quasiparticle is effected about a localized quasiparticle in order to probe their mutual exchange statistics. The Aharonov–Bohm phase between two quasiparticles may be induced by varying the magnetic flux by changing either the magnetic field or the area enclosed by the trajectory. An even–odd effect with respect to the number of localized non-Abelian quasiparticles can indicate the existence of the non-Abelian statistics [8, 9].

Studies of mesoscopic Fabry–Perot interferometers fabricated from high-mobility GaAs/AlGaAs heterostructures have detected anomalous Aharonov–Bohm-like (ABL) interference in the quantum Hall regime [10–12]. These periodic magneto-oscillations have been interpreted either as a consequence of zero-dimensional states formed as a result of constructive interference of one-dimensional (1D) electron waves traveling along the edge channels [10] or as the Aharonov–Bohm interference of edge electrons [11]. Similar data in the FQH regime have been interpreted as the interference of Laughlin quasiparticles due to fractional statistics [12]. More recent studies of Fabry–Perot interferometers have uncovered the size and interaction effects of ABL oscillations [13, 14]. Signals detected at $5/2$ filling have been interpreted as the even–odd effect of non-Abelian quasiparticles [15, 16].

In this paper, our study of a quantum Hall interferometer fabricated from an ultra-high-mobility GaAs/AlGaAs quantum well is reported. The interferometer features a pair of narrow constrictions through which a circular disc of electrons is connected to the bulk 2D electron system. Magnetotransport in the quantum Hall regime reveals a set of prominent, periodic oscillations reminiscent of the Aharonov–Bohm effect. From the flux period scaling, the effective area of the interferometer and the flux period of Φ_0/f, where f is the integral value of fully filled Landau levels through the constrictions, have been self-consistently

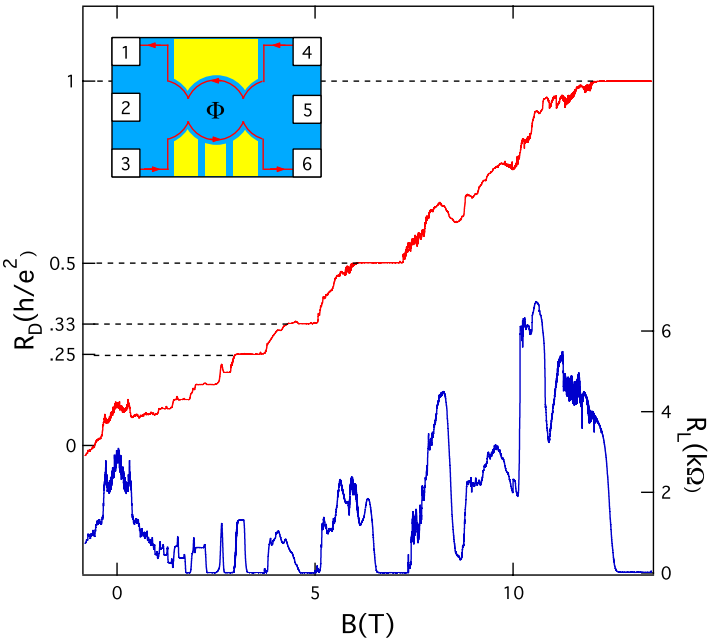

Figure 1. The longitudinal, R_L, and diagonal, R_D, magnetoresistances of a Fabry–Perot interferometer ($T < 10$ mK). The inset shows the layout of the interferometer. The red lines show the edge state trajectory. A source–drain current is applied across contacts 2–4, the longitudinal magnetoresistance is measured across contacts 3–6, and the diagonal magnetoresistance is measured across contacts 1–6.

determined. Our findings are mostly in agreement with the predictions on the Coulomb-dominated model of quantum Hall interferometers [17, 18]. Recent experiments have also drawn similar conclusions [13, 14].

2. Experimental

The Fabry–Perot interferometer was fabricated from a high-mobility, symmetrically doped GaAs/AlGaAs quantum well. The low-temperature mobility of the unprocessed sample was $28.3 \times 10^6\,\mathrm{cm}^2\,(\mathrm{Vs}^{-1})$ with an electron density of $n = 3.3 \times 10^{11}\,\mathrm{cm}^{-2}$. The layout of the interferometer is shown in the inset of figure 1. The interferometer was initially defined using e-beam lithography, dry etched to the depth of the 2D electron system, and metalized with TiAu prior to lift-off. The diameter of the interferometer is $1.2\,\mu$m, and the width of the two constrictions is $\sim$400 nm. The sample was mounted on a dilution refrigerator capable of reaching less than 10 mK. Depletion induced by the etched sidewalls reduces the electron density in the constrictions, n_c, by $\sim$11% relative to the bulk density, n_b. As a result, ν_c, the filling factor across the constrictions, is smaller than ν_b, the bulk filling factor [19].

3. Results

Figure 1 illustrates the longitudinal, R_L, and the diagonal, R_D, magnetoresistances of the interferometer at temperatures below 10 mK and at magnetic fields ranging from –1 to 13 T.

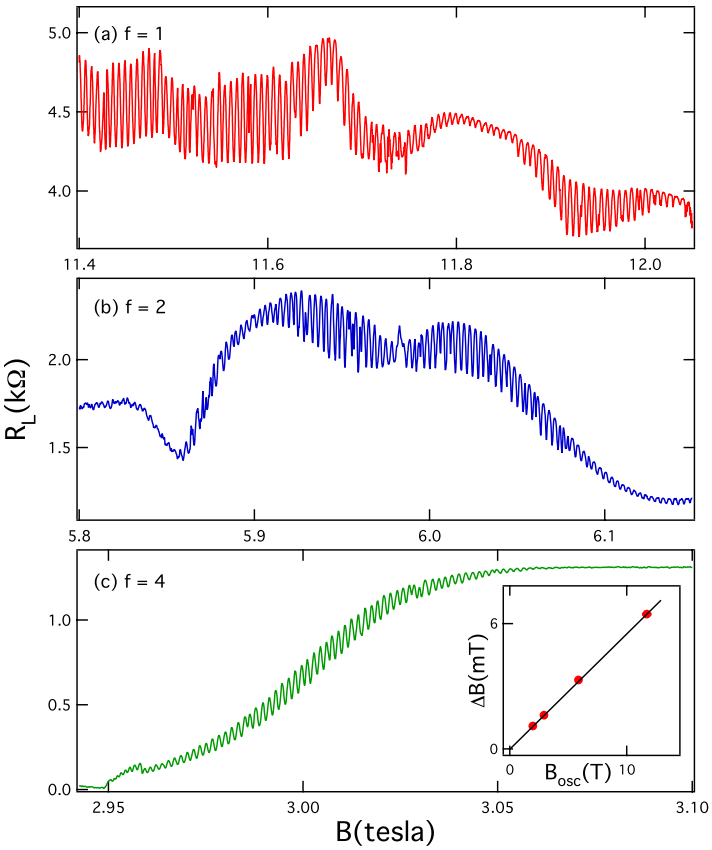

Figure 2. Periodic oscillations in the longitudinal magnetoresistance, R_L, on the low field side of the (a) $\nu_c = 1$, (b) $\nu_c = 2$ and (c) $\nu_c = 4$ plateaus. Inset of (c): dependence of the period of ABL oscillations, ΔB, on B_{osc}, the magnetic field at which they occur.

The low-field ($|B| < 1$ T) fluctuations arise as a consequence of the interference of ballistic paths in confined devices whose mean free path exceeds the dimensions of the device [20]. Above $B > 1$ T, a number of zero-resistance regions in R_L and plateaus in the R_D define the quantum Hall state. As revealed by the R_L minima and the R_D plateau, strong quantum Hall states are detected at $\nu_c = 1$, 2, 3, 4 and 6. From the overlap of the Hall plateaus in R_D and the vanishing R_L, we find that the $\nu_b = \nu_c$ overlap occurs for these quantum Hall states. Such an overlap is not seen for other quantum hall states as $\nu_c \neq \nu_b$ due to density gradient [21, 22][6].

Figure 2 illustrates the ABL oscillations that are observed in R_L on the low-field side of the $\nu_c = 1$, 2 and 4 plateaus, with the ABL oscillations below the $\nu_c = 1$ and 2 plateaus being the strongest. The amplitude of the ABL oscillation in R_L can be $\geqslant 15\%$ of the background resistance for $\nu_c = 1$ and 2 ABL oscillations. Depending on the temperature and thermal cycling, over $\geqslant$300 periods can be detected for a single set of ABL oscillations. Interestingly, no

[6] Analysis of the transport through the quantum point contacts in Fabry–Perot interferometers within the Landauer–Buttiker formalism [21, 22] yields a longitudinal magnetoresistance $R_L = (\frac{1}{\nu_c} - \frac{1}{\nu_b})\frac{h}{e^2}$ and diagonal resistance $R_D = \frac{1}{\nu_c}\frac{h}{e^2}$, where ν_c and ν_b are the filling factors at the constrictions and bulk, respectively.

Table 1. Properties of the first four largest sets of ABL oscillations. ΔB is the period of oscillations (with variance of ΔB shown for $f = 1$ and 2 oscillations), $B_{\rm osc}$ is the center of the oscillation range, $\Delta B_{\rm osc}$ is the range of oscillations, f is the integer number of the fully filled Landau levels in the constrictions, and $r = \sqrt{\Phi_0/\pi f \Delta B}$ is the radius of the area of flux quantization.

ΔB(mT)	6.45 ± 0.18	3.30 ± 0.24	1.61	1.09
$B_{\rm osc}$(T)	11.71	5.89	2.94	1.97
$\Delta B_{\rm osc}$(T)	1.20	0.60	0.16	0.06
$\Delta B_n/\Delta B_1$	1	0.51	0.25	0.17
$B^n_{\rm osc}/B^1_{\rm osc}$	1	0.50	0.25	0.17
$1/f$	1	1/2	1/4	1/6
r(nm)	452	447	452	449

oscillations are detected on the low-field side of the $\nu_{\rm c} = 3$, 5 and other odd integer plateaus. At lower temperatures, ABL oscillations even for $\nu_{\rm c} \leqslant 10$ have been detected [19].

The inset of figure 2(c) shows the linear dependence of the ABL oscillation period ΔB as a function of $B_{\rm osc}$, the center of the magnetic field range in which the periodic oscillations are found. The values of ΔB and $B_{\rm osc}$ scale in a way that yields the ratio of $1{:}\frac{1}{2}{:}\frac{1}{4}{:}\frac{1}{6}$ between the first four sets of oscillations. Such a scaling of ΔB and $B_{\rm osc}$ always yields the number of fully filled Landau levels, f, or equivalently the quantum number of the quantized Hall plateaus in $R_{\rm D}$ with the ABL oscillations appearing on the low field side. Table 1 summarizes the properties of ABL oscillations from the data shown in figures 1 and 2. Similar scaling of ΔB and $B_{\rm osc}$ has been reproduced under different illumination and cool-down conditions [19].

For a Fabry–Perot interferometer of radius r, the enclosed flux is $\Phi = B\pi r^2$. From the scaling of the magnetic field periods in table 1, the period ΔB of the ABL oscillations is phenomenologically related to the flux period by $\Delta B \pi r^2 = \Phi_0/f$. As shown in table 1, the radius calculated for each ΔB consistently yields $\sim$450 nm as the radius of the interferometer. An active radius of 450 nm appears to be reasonable for the interferometer with a diameter of 1.2 μm once the effect of sidewall depletion is taken into account. It is notable that Φ_0/f is the flux period even though the $f + 1$st Landau level is partially occupied within the constriction.

4. Discussion

An intriguing feature of a Fabry–Perot interferometer is that it exhibits an extended sequence of ABL oscillations in the second Landau level. Figure 3(a) shows $R_{\rm D}$ with ABL oscillations beginning immediately on the low field side of the $\nu_{\rm c} = 2$ plateau and lasting until nearly the $\nu_{\rm c} = 3$ plateau. Figure 3(b) shows $\Delta R_{\rm D}$, which is $R_{\rm D}$ with the smooth background subtracted. $\Delta R_{\rm D}$ shows apparent amplitude modulation with the strongest oscillations found just below the $\nu_{\rm c} = 2$ plateau. Figure 3(c) shows the magnetic field period ΔB determined from $\Delta R_{\rm D}$ data in figure 3(b). Each period was determined by the Fourier analysis of a different window of the magnetic field. A reduction of 10% in ΔB between $\nu_{\rm c} = 2$ and 3 is found with some scatter. Changing periods may mean that different areas are being probed. Indeed, there is a sudden change where $\nu_{\rm c} \approx 5/2$, where one might expect a rearrangement of densities in the interferometer due to the condensation of the 5/2 state.

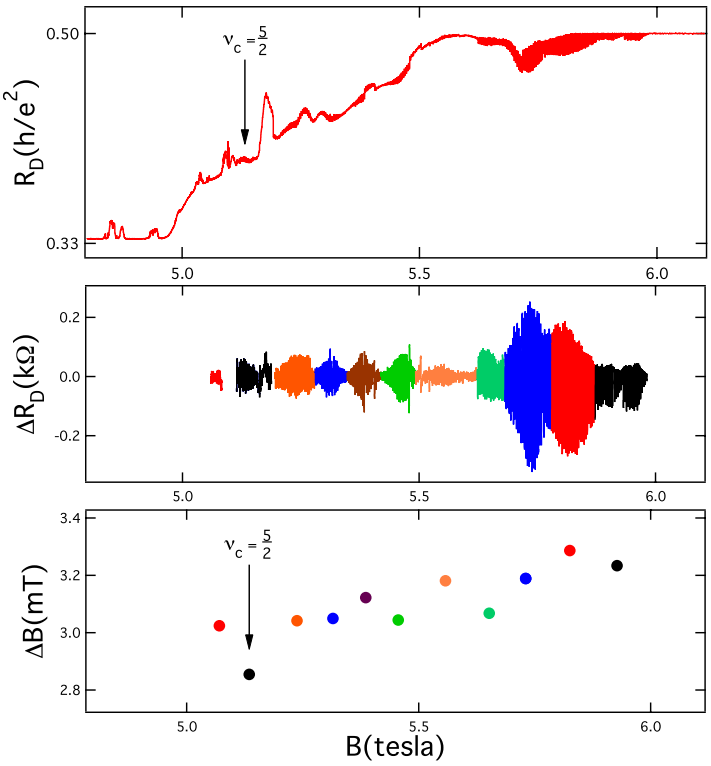

Figure 3. (a) Diagonal resistance between $\nu_c = 2$ and 3 under a different illumination condition than figure 1. (b) Expanded view of the oscillations with background resistance subtracted. (c) Oscillation periods in the second Landau level.

Figure 4 illustrates the striking asymmetry between the low and the high field sides of the $\nu_c = 2$ plateau. The conductance $G = 1/R_D$ shows a particularly strong set of ABL oscillations on the low magnetic field side of the $\nu_c = 2$ plateau. The upper inset of figure 4 shows an expanded view of G on the immediate, low field side of the $\nu_c = 2$ plateau. A series of equally spaced, Coulomb blockade-like conductance peaks is observed as the magnetic field is reduced from the $\nu_c = 2$ plateau. The lower inset of figure 4 shows an expanded view of conductance on the high magnetic field side of the $\nu_c = 2$ plateau. Unlike the low field side, there are no ABL oscillations as the conductance exhibits irregular, jagged dips. Fourier analysis shows no dominant oscillation frequency.

Our experiment establishes the following notable features of ABL oscillations: (i) ABL oscillations are observed only on the low magnetic field side of the $\nu_c = 1$, 2, 4, 6 and other even integer Hall plateaus. Except below the $\nu_c = 1$ plateau, ABL oscillations are noticeably absent below odd integer Hall plateaus. (ii) No ABL oscillations are observed on the immediate, high field side of Hall plateaus. (iii) The ABL oscillations possess a flux period of Φ_0/f where f is the number of fully filled Landau levels. The $f + 1$st Landau level is partially occupied within the constrictions. (iv) A typical set of oscillations terminates within 300 periods or less. (v) Below the $\nu_c = 2$ plateau, the ABL oscillations persist over nearly the entire second Landau level. (vi) The ABL oscillations can be detected even when the constriction is in a compressible state, i.e. there is no quantized Hall state. This is most clear below the $\nu_c = 1$ and 2 plateaus.

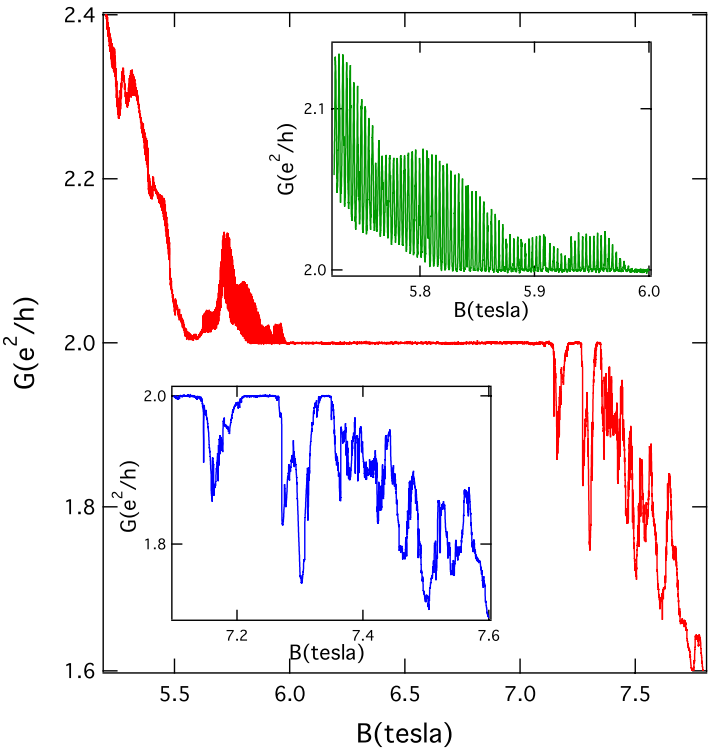

Figure 4. Conductance of the Fabry–Perot interferometer between filling factors $\nu_c = 1.6$ and $\nu_c = 2.4$. Upper (lower) inset: expanded view of conductance on the low (high) magnetic field side of the $\nu_c = 2$ plateau.

The features noted above establish that the ABL oscillations are not from the Aharonov–Bohm effect, which possesses a flux period of Φ_0 and two copropagating interference trajectories. Similarly, the non-interacting model of [10] predicts a flux period of Φ_0 and is not consistent with our results. In contrast, our findings are mostly in agreement with the Coulomb-dominated model of quantum Hall interferometers proposed by Rosenow and Halperin [17, 18]. In the simplest version of this model, the constriction consists of an incompressible fluid at integer filling fraction f and the interferometer contains a compressible island at somewhat higher density. Transport through the system is effected by (A) forward tunneling from the bulk through the island, (B) backscattering from the edge state through the island and (C) backscattering between edge states via tunneling at the constrictions.

The first two processes (A and B) occur via tunneling through the center island and are enhanced when the Coulomb blockade condition is satisfied, i.e. when the energy of N and $N+1$ electrons on the island is equal. Since the constrictions are quantized at the filling fraction f, the addition of a flux quantum Φ_0 transports f electrons into the central compressible island region, satisfying the Coulomb blockade condition f times. Thus these processes show oscillating conductivity with a magnetic flux period of Φ_0/f.

On the lower magnetic field side of the plateau, the Rosenow–Halperin model predicts that either forward tunneling from the bulk (A) or backscattering from the edge (B) should be predominant. The positive conductance peaks shown in the low field side of the $\nu_c = 2$ plateau shown in figure 4 identify each peak as a forward tunneling event that increases the

overall conductance. Below the $\nu_c = 1$, 2, 4 and 6 plateaus, conductance uniformly increases, suggesting predominance of forward scattering in the ABL oscillations immediately below these Hall plateaus.

On the high field side of Hall plateaus, the model [17] favors backscattering via either tunneling through the island (B) or tunneling at the constrictions (C). Since backscattering reduces the overall conductance, the negative conductance features found above the $\nu_c = 2$ plateau shown in figure 4 can be interpreted as a sign of backscattering.

In particular, we cannot identify any particular region as being due to interferences associated with process (C). It is, of course, possible that the complicated and irregular nature of the signal is a result of several competing processes.

A salient feature of the ABL oscillation is that it is detected below the $\nu_c = 1$, 2, 4, 6 and other even integer Hall plateaus, but not below other odd plateaus. Clearly, spin plays a non-trivial role in whether or not ABL oscillations can be observed. This is likely because the smaller exchange gap for odd integers (compared with the cyclotron gap of even integers) makes the physical distance between the $2n$–1 and $2n$ edges smaller than that between the $2n$ and $2n + 1$ edges. Thus, in the forward scattering process (A), the distance required for a particle to tunnel from the bulk to the island could be smaller on the low field side of an even plateau than on the low field side of an odd plateau.

In contrast to the model described by Rosenow and Halperin [17], we detect ABL oscillations when the filling factors inside the constrictions are in a compressible regime. Indeed, for the ABL below $\nu = 2$, roughly the same period oscillations are seen almost all the way to $\nu = 3$. While this is slightly outside of the orthodox model, it allows us to conclude that throughout this region, (a) the tunneling is always single-electron tunneling; (b) the oscillations are from a Coulomb-dominated origin; and (c) the addition of a flux quantum Φ_0 continues to add an integer number of f electrons to the island, even though the constriction may have a partially filled $f + 1$st Landau level. If the constriction is really quantized at filling ν_c, the addition of a flux quantum is expected to add charge $\nu_c e$. However, this does not appear to be the case.

5. Conclusion

In summary, we have studied the ABL oscillations in a Fabry–Perot interferometer in the quantum Hall regime. The ABL oscillations are most prominent in the low field side of the $\nu = 1, 2, 4, 6, \ldots$, quantum Hall plateaus. They can be detected over extended ranges of magnetic fields, including over the compressible filling factors. Their flux period is Φ_0/f, where f is the integral value of fully filled Landau levels through the constriction. These features establish that Φ_0/f ABL oscillations do not arise from the conventional Aharonov–Bohm effect. Instead, these oscillations can be identified as electron tunneling peaks due to the Coulomb-dominated process through the island formed inside the interferometer. Efforts to extend Fabry–Perot interferometry to the $\nu = 5/2$ FQH are currently in progress.

Acknowledgments

We thank N Cooper, F D M Haldane, N P Ong, S Sondhi, D C Tsui and A Yazdani for useful discussions. This work was supported by the Microsoft Q Project and the University of Chicago MRSEC.

References

[1] Nayak C, Simon S H, Stern A, Freedman M and Das Sarma S 2008 *Rev. Mod. Phys.* **80** 1083
[2] Das Sarma S, Freedman M and Nayak C 2005 *Phys. Rev. Lett.* **94** 166802
[3] Willett R, Eisenstein J P, Stormer H L, Tsui D C, Gossard A C and English J H 1987 *Phys. Rev. Lett.* **59** 1776
[4] Pan W, Xia J-S, Shvarts V, Adams D E, Stormer H L, Tsui D C, Pfeiffer L N, Baldwin K W and West K W 1999 *Phys. Rev. Lett.* **83** 3530
[5] Xia J S, Pan W, Vicente C L, Adams E D, Sullivan N S, Stormer H L, Tsui D C, Pfeiffer L N, Baldwin K W and West K W 2004 *Phys. Rev. Lett.* **93** 176809
[6] Moore G and Read N 1991 *Nucl. Phys.* B **360** 362
[7] Read N and Rezayi E 1996 *Phys. Rev.* B **54** 16864
[8] Stern A and Halperin B I 2006 *Phys. Rev. Lett.* **96** 016802
[9] Bonderson P, Kitaev A and Shtengel K 2006 *Phys. Rev. Lett.* **96** 016803
[10] van Wees B J, Kouwenhoven L P, Harmans C J P M, Williamson J G, Timmering C E, Broekaart M E I, Foxon C T and Harris J J 1989 *Phys. Rev. Lett.* **62** 2523
[11] Camino F E, Zhou W and Goldman V J 2005 *Phys. Rev.* B **72** 155313
[12] Camino F E, Zhou W and Goldman V J 2005 *Phys. Rev. Lett.* **95** 246802
[13] Zhang Y, McClure D T, Levenson-Falk E M, Marcus C M, Pfeiffer L N and West K W 2009 *Phys. Rev.* B **79** 241304
[14] Ofek N, Bid A, Heiblum M, Stern A, Umansky V and Mahalu D 2010 *Proc. Natl Acad. Sci. USA* **107** 5276
[15] Willett R L, Pfeiffer L N and West K W 2009 *Proc. Natl Acad. Sci. USA* **106** 8853
[16] Willett R L, Pfeiffer L N and West K W 2010 *Phys. Rev.* B **82** 205301
[17] Rosenow B and Halperin B I 2007 *Phys. Rev. Lett.* **98** 106801
[18] Halperin B I, Stern A, Neder I and Rosenow B 2010 arXiv:1010.4598
[19] Choi H *et al* unpublished work
[20] Marcus C M, Rimberg A J, Westervelt R M, Hopkins P F and Gossard A C 1992 *Phys. Rev. Lett.* **69** 506
[21] Washburn S, Fowler A B, Schmid H and Kern D 1988 *Phys. Rev. Lett.* **61** 2801
[22] Beenakker C W J and van Houten H 1991 Quantum transport in semiconductor nanostructures *Solid State Physics* vol 44, ed H Ehrenreich and D Turnbull (San Diego, CA: Academic) pp 1–228